

Contents lists available at [ScienceDirect](https://www.sciencedirect.com)

Journal of Hydrology: Regional Studies

journal homepage: www.elsevier.com/locate/ejrh

MODIS (2001-2022) snow cover variability over the Italian territory

Veronica Manara^a, Cecilia Delia Almagioni^{a,b}, Guglielmina Adele Diolaiuti^a,
Maurizio Maugeri^{a,c}, Davide Fugazza^{a,*}

^a Department of Environmental Science and Policy, University of Milan, via Celoria 10, Milan 20133, Italy

^b Department of Physics "Aldo Pontremoli", University of Milano, via Celoria 16, Milan 20133, Italy

^c Institute of Atmospheric Sciences and Climate, CNR, Bologna, Italy

ARTICLE INFO

Keywords:

ERA5-Land

Snow cover duration

Climatology

Trend analysis

Snow-elevation relationship

ABSTRACT

Study region: The Italian territory including the southern part of the Alps and the Apennine chain.
Study focus: The snow cover variables (duration – SCD, onset – SOD, end - SED) have been analysed between 2000 and 2022 using MODIS data to study their spatial distribution and temporal evolution. The snow cover extent (SCE) obtained from ERA5-Land has been used to evaluate trends over a longer period (since 1950s).

New hydrological insights for the region: The spatial distribution of SCD shows a dependence on elevation (76 % variance explained); high variability at each elevation is also seen, underlining the importance of other parameters (e.g., slope, aspect, longitude, latitude). A similar pattern is observed for SOD and SED. The SCD series for Italy shows very high interannual variability resulting in a significant negative trend (between -5.1 and -0.6 days decade⁻¹) at elevations > 3500 m a.s.l., owing to the signal observed over the Alps. A good agreement (correlation=0.91) is found between the temporal evolution of SCD from MODIS and the SCE obtained from ERA5-Land allowing to evaluate the trend since the 1950s which was found negative (-4 % decade⁻¹) and significant over the Italian territory owing to the decreasing SCE in the Alpine region. The obtained results are important in view of the socioeconomic importance of snow cover for the considered area for agriculture, human consumption, tourism and industry sector.

1. Introduction

Snow cover plays an essential role in regulating the Earth's climate and thus any change in it can contribute to alterations in the climate system. When snow melts, as a direct effect of a lower albedo of the surface, a lower fraction of solar radiation is reflected, and a higher fraction is absorbed by the Earth increasing its temperature, an effect known as snow-albedo feedback. This effect amplifies the increase of the Earth's temperature due to the increase in greenhouse gas (Flanner et al., 2011; Thackeray et al., 2019; Young, 2023).

Beside this large-scale effect, snow cover has significant impacts on human well-being in several parts of the world. As a source of freshwater used for agriculture and human consumption, snowmelt is a major provisional ecosystem service, particularly in arid regions of Asia (Su et al., 2019) but also in Europe and North America, and approximately 2 billion people are at risk of decreased water supply from changing snowmelt patterns in the coming century (Mankin et al., 2015). Meltwater from snow also constitutes a large

* Corresponding author.

E-mail address: davide.fugazza@unimi.it (D. Fugazza).

<https://doi.org/10.1016/j.ejrh.2025.102895>

Received 29 May 2025; Received in revised form 24 October 2025; Accepted 26 October 2025

2214-5818/© 2025 The Author(s). Published by Elsevier B.V. This is an open access article under the CC BY-NC-ND license (<http://creativecommons.org/licenses/by-nc-nd/4.0/>).

share of the annual discharge used as a source of energy for hydroelectric power, particularly in the Alps (D'Agata et al., 2018) and Scandinavian Mountains (Engelhardt et al., 2014). Natural snow cover further influences the economic revenue of ski resorts (Rixen et al., 2011) and can function as a habitat for plant (Keller et al., 2005) and animal species (Gilbert et al., 2017), determining the migration patterns of wildlife and their survival (Deshpande et al., 2022). Along with these beneficial effects, snow melt can however also constitute a source of natural hazards when excess meltwater leads to flooding causing loss of lives and property, as experienced by local communities in parts of Central Asia (Fugazza et al., 2020).

As the amount of precipitation that falls as rain or snowfall is influenced by air temperature, which also has an impact on snow melt patterns, the presence of snow on the ground is highly sensitive to changes in the Earth's climate; in the northern hemisphere, Mudryk et al. (2020) observed a decrease in snow cover extent in all months between 1981 and 2018, largest in November, December, March and May, from a multi-dataset ensemble of gridded observational dataset. Kunkel et al. (2016) also observed lower snow cover extent during 1992–2015 compared to 1967–1991 from the analysis of weekly snow cover maps produced by NOAA. The changes are particularly pronounced in spring, reflecting earlier snow melt, as opposed to the onset of snow cover in autumn.

The creation of a climatology of snow cover duration, and the assessment of trends in this variable, can be carried out using a network of station observations, remote sensing, or a combination of both (Kunkel et al., 2016; Mudryk et al., 2020). While station observations usually provide the longest records, allowing to reconstruct trends going back to the middle of the 20th century (Brown et al., 2021; Matiu et al., 2021; Valt and Cianfarra, 2010), and even further back (Diodato et al., 2020), they often suffer from issues related to data quality, homogeneity and representativeness of the stations with respect to their surroundings. In contrast, remote sensing can provide data distributed on a regular grid although often at the cost of a limited temporal outlook or coarse grid size (Bormann et al., 2018) as well as other limitations like cloud obstruction, the difficulty of distinguishing between clouds and snow cover and the topographic shading, which is true in particular in areas with complex orography. Northern hemisphere snow cover trends since the 1960s are often assessed using the NOAA snow cover maps, with a grid size of 190.6 km at 60° latitude (Estilow et al., 2015). Investigations at the region or country scale require higher spatial resolution and can be carried out using observations from AVHRR, available from the 1980s or MODIS, available from 2000. Such products have been used to create snow cover duration climatologies over Europe (Dietz et al., 2012) and assess trends in this variable over the Alpine region (Fugazza et al., 2021; Hüsler et al., 2014). Besides ground stations and remote sensing imagery, reanalysis datasets such as ECMWF-ERA5 (Hersbach et al., 2020) and ERA5-Land (Muñoz-Sabater et al., 2021) also provide snow cover variables; reanalysis products have the advantages of a long temporal duration (e.g. ERA5 is available since 1940) and of yielding the data on a distributed grid without missing data, although at a coarser size compared to e.g. MODIS (0.1 × 0.1° for ERA-5 land), even if high-resolution products are considered. Comparison between snow cover variables from ERA5 and ERA5-Land and satellite products generally shows good agreement as concerns the snow cover extent (SCE), while biases have been detected in the ability of reanalysis products to correctly represent snow water equivalent (Kouki et al., 2023). In Italy, snow cover is an important resource for agriculture, human consumption, the energy and tourism sectors (Colombo et al., 2023). In 2021, gross production of hydroelectric energy in the country accounted for 47 TWh, i.e. 16 % of the total electric energy generated, and 51 % of electricity produced from renewable sources (Terna, 2021). Most hydroelectric plants are located in the northern part of the country, where snow contributes a large share of annual discharge, with peaks above 70 % in high altitude catchments during late spring-early summer (Soncini et al., 2017; Stucchi et al., 2019). Concerning winter tourism, Italy has 349 ski resorts, which hosted more than 20 million visitors in 2021. The market is made up of many small operators, spread throughout the country from the northern regions to Sicily and Sardinia (Vanat, 2022); research shows that these small operators are more at risk of loss of revenues from declining snow cover duration compared to the larger players (Moreno-Gené et al., 2018).

In spite of the economic relevance of snow for the country, the last study describing the distribution of snow cover duration over the whole territory is related to the period 1921–1960 (Gazzolo and Pinna, 1973). Since then, although several studies have analysed in detail the distribution and temporal evolution of snow cover duration over the Italian Alps and northern regions, using station observations and satellite data (Fugazza et al., 2021; Godone et al., 2011; Terzago et al., 2010), central and southern Italy have received comparatively less attention, in spite of several months of snow coverage in the Apennines (Annella et al., 2023; Capozzi et al., 2025). As Italy, and particularly its southern regions, is frequently affected by drought episodes (Buttafuoco and Caloiero, 2014; Pascale and Ragone, 2025), analysing spatial and temporal patterns of snow cover variables over the Italian territory has become increasingly important for the management of the country's water resources.

In this study, we analyse the distribution of snow cover variables over the whole Italian territory which includes the southern part of the Alps and the Apennines (Section 2.1) between 2000 and 2022 using MODIS data acquired from Terra and Aqua platform. After a pre-processing of the data (Sections 2.2 and 2.3) in order to obtain for each pixel a binary field (snow or snow free), the onset, the duration and the end of the snow cover season have been calculated (Section 2.4). We aim to provide both a climatology of snow cover duration (Section 3.1), discussing its relationship with geographical parameters (Section 3.2) and analyse the temporal evolution of snow cover variables (Section 3.3 and Section 3.4) in the Italian peninsula over the past two decades. Then, a discussion (Section 4) of the results considering also the snow cover extent from ERA5-Land over the common period and over the whole available period (1950–2022) is performed. Finally, some conclusions on the obtained results are outlined (Section 5).

2. Materials and methods

2.1. Study area

The area analysed in this study is the Italian territory (Fig. 1). It includes the southern side of the Alps and the Apennines with elevations reaching 4810 m a.s.l. (4676 m a.s.l. at 500 m spatial resolution) and with an average elevation equal to about 630 m

(Fig. 2). We further identified 5 subregions defined following a hydrographic approach to investigate the spatial variability of the snow cover and its links to the geographic variables. Specifically, we divided the Italian territory in the Alps region (delimited by the Italian political border in the north and by the Po basin in the south and thus including the southern part of the Alps chain, the Po plain and the northern part of the Apennines chain), Apennines west and east regions (delimited by the Po Basin in the north and divided in two areas considering the watershed divide), Sicily and Sardinia regions.

2.2. Snow cover data and ancillary data

To identify snow-covered pixels, we used data from the MODIS Terra Snow Cover Daily L3 Global 500 m SIN Grid V061 (MOD10A1 V61) and MODIS Aqua Snow Cover Daily L3 Global 500 m SIN Grid V061 (MYD10A1 V61) products (Hall and Riggs, 2021a, 2021b), generated by the US National Snow and Ice Data Center (NSIDC) at approximately 500 m resolution. All the daily scenes for the tiles containing the Italian territory (h18v04, h18v05, h19v04, h19v05) from both satellites were downloaded for the 2000–2022 period. MOD10A1 scenes are processed from the data acquired by MODIS onboard Terra platform, with a morning overpass (around 10:30 a. m. at the equator), while MYD10A1 scenes are processed from the data acquired by MODIS onboard AQUA platform, with an afternoon

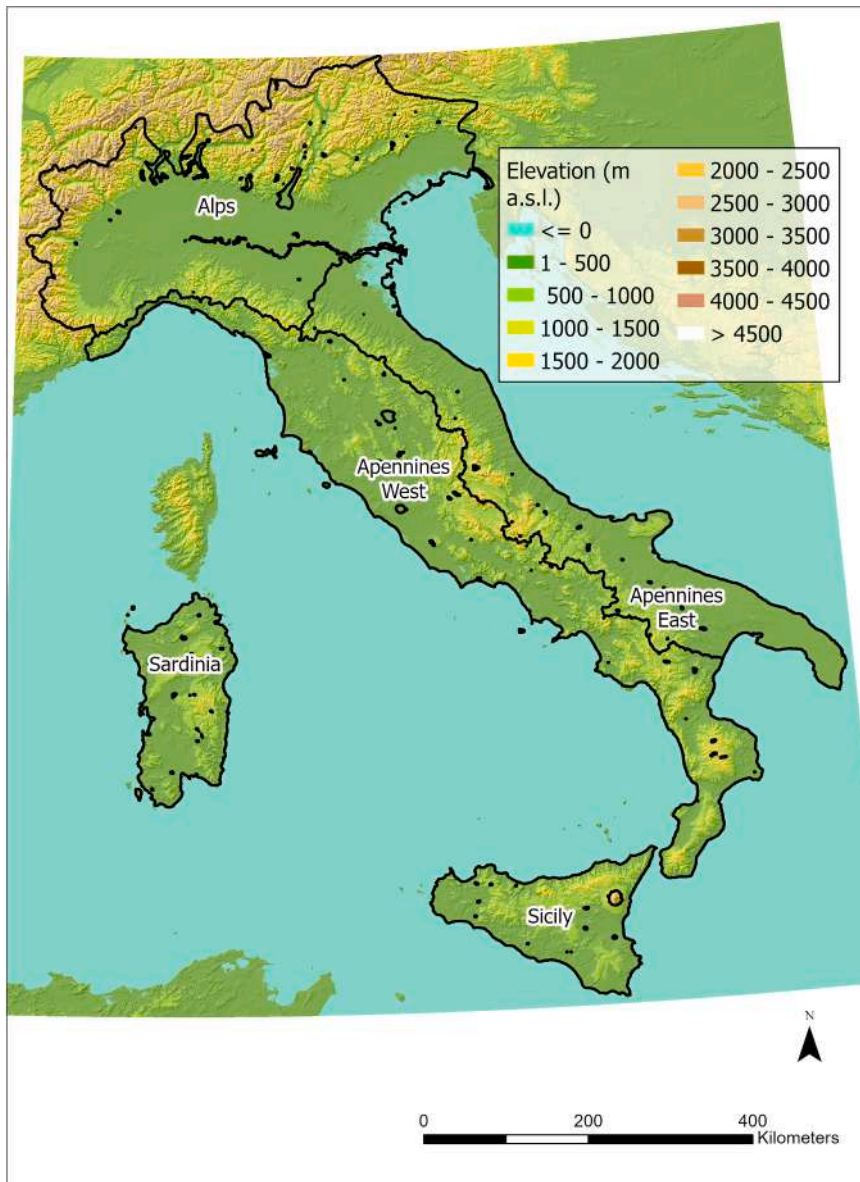


Fig. 1. Topography of the study area. The borders of the 5 sub-regions are also shown. Source of elevation data is the ALOS AW3D30 global digital elevation model resampled to 500 m spatial resolution.

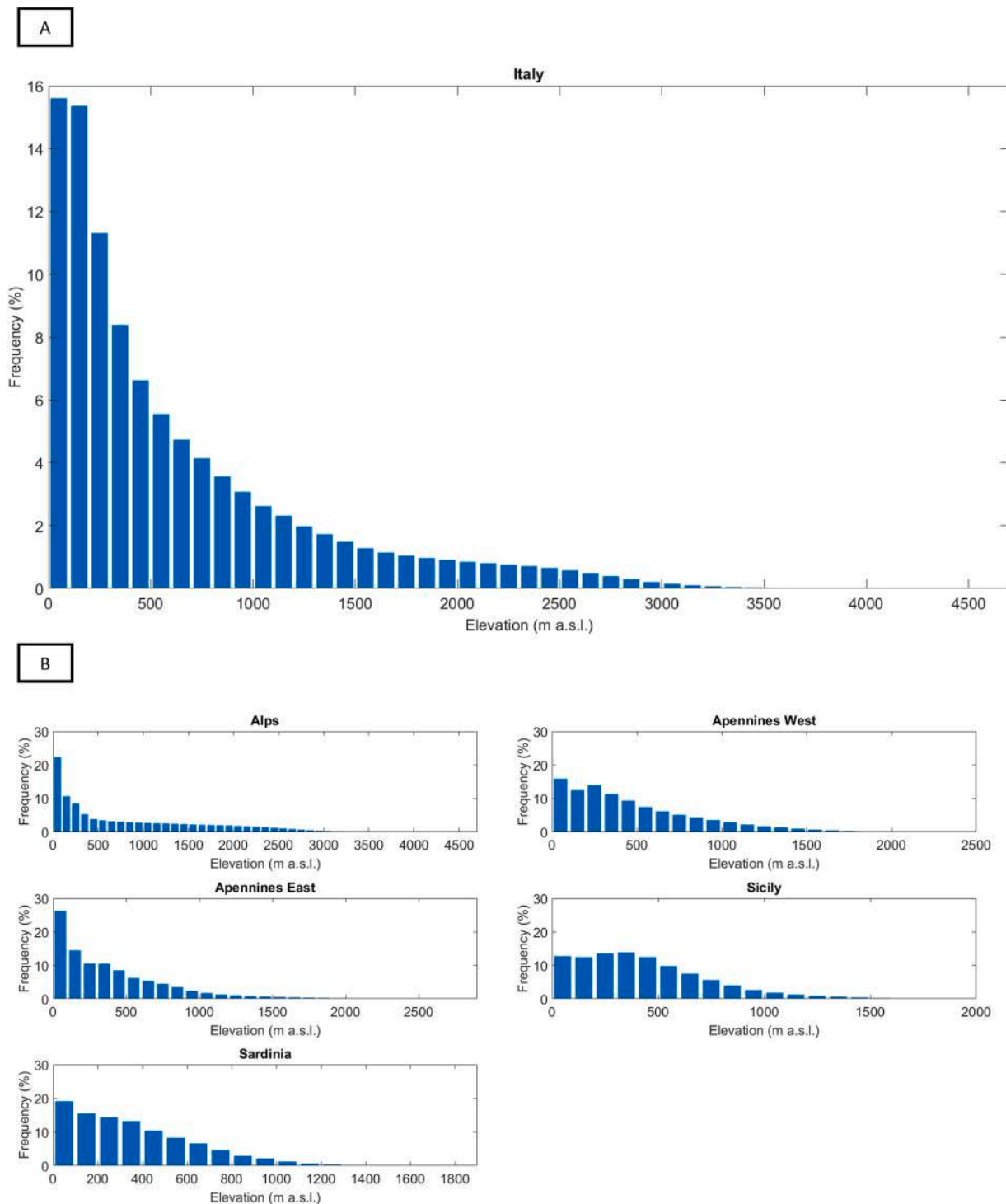


Fig. 2. Frequency distribution of elevation in the study area (a) and in the 5 sub-regions (b) for a bin length of 100 m. Source of elevation data is the ALOS AW3D30 global digital elevation model resampled to 500 m spatial resolution.

overpass (about 1:30 p.m. at the equator). The algorithm that allows to establish if a pixel is covered by snow or by another type of surface takes advantage from the fact that snow has very high reflectance in the visible part of the spectrum and very low reflectance in the shortwave infrared. This characteristic is exploited by the normalized difference snow index (NDSI), which uses reflected solar radiation in the visible (band 4, 0.545–0.565 μm) and in the shortwave infrared (band 6, 1.628–1.672 μm for MODIS Terra; band 7,

2.105–2.155 μm for Aqua) to increase the contrast between snow-covered and snow-free surfaces (Eq. 1):

$$NDSI = \frac{\text{band4} - \text{band6}(7)}{\text{band4} + \text{band6}(7)} \quad (1)$$

Specifically, a value of NDSI lower than or equal to 0 means that the pixel is free from snow while a value of NDSI higher than 0 means that the pixel is covered at least partly by snow. It is important to underline that all the pixels covered by snow have a positive NDSI but a positive NDSI does not mean that the pixel is covered by snow. This can happen for examples to pixels covered by clouds or fresh water like rivers and lakes. At the same time, the NDSI value can be lowered by the presence of vegetation.

For the analysis presented in this paper, the NDSI_Snow_Cover product is used by merging the four individual tiles for both satellites and reprojecting the merged product into the WGS84 coordinate system.

In this product, a pixel can be classified as free from snow, covered by snow (specifying the corresponding NDSI value), covered by fresh water, located in the sea, covered by clouds, recorded during the night (when lighting conditions are not sufficient), missing or classified as undecided. First, the complexity of the dataset was decreased by classifying as missing data all the data of the pixels covered by clouds, recorded during the night or classified as undecided. Moreover, all the pixels located in the sea are not considered in the analysis and the pixels classified as covered by fresh water are managed as follows: a pixel classified as covered by fresh water for at least 10 % of the days in the whole considered period was considered as a fresh water pixel (lakes and rivers) and it was not considered in the analysis, while in the other cases, the pixel was considered but the data recorded as covered by fresh water were considered as missing data. Finally, all the pixels with NDSI lower than 0.4 are considered free from snow and those with NDSI higher than 0.4 (Salomonson and Appel, 2006) as covered by snow. After this step, the data used in the analysis can be classified by means of only three entries: free from snow, covered by snow or missing.

To identify the elevation of the pixels considered in the analysis, the ALOS (Advanced Land Observing Satellite) Global Digital Surface Model “ALOS World 3D-30m (AW3D30)” Digital Elevation Model (Tadono et al., 2014) with a resolution of 30 m was used, reprojected to WGS84 as done for the MODIS products. Finally, monthly snow cover extent values from ECMWF-ERA5 Land reanalysis dataset are used (Muñoz-Sabater et al., 2021). This dataset is available with a resolution of $0.1^\circ \times 0.1^\circ$ since 1950, allowing to compare snow cover information with MODIS over the common period and to reconstruct the evolution of snow over a longer period.

2.3. Gap filling

In order to fill the missing values in the MODIS data and obtain a value (snow or snow-free) for each pixel, the methodology proposed by Gafurov and Bárdossy (2009) and adapted by Almagioni et al. (2025) and Fugazza et al. (2021) was used. It is based on the combination of six steps (for more details see Fugazza et al., 2021):

- 1) Combination of Terra and Aqua products from the same day. If a pixel on one day is cloud covered in the MOD10A1 (Terra) product and is snow covered/snow free in the MYD10A1 (Aqua) product, the value from MYD10A1 is retained.
- 2) Temporal combination of adjacent dates. If a pixel on a given day is cloud covered and is snow covered (snow-free) on the previous and next day, it is considered snow covered (snow-free).
- 3) Snow transition elevation. In this step, the elevation of the maximum snowline (above which all pixels are snow covered) and minimum snowline (below which all pixels are snow free) is calculated for each sub-region. A cloudy pixel is considered snow covered if its elevation lies above the maximum snowline and snow free if it is below the minimum snow line. This step is applied if the cloud cover in a given sub-region is below 30 %.
- 4) Spatial interpolation. The four pixels around the selected pixel are considered; if at least three of these pixels are snow-covered (snow-free), the given pixel is considered snow-covered (snow-free).
- 5) Combination of spatial interpolation with elevation of surrounding pixels. The 3×3 neighbourhood of each pixel is considered; the central pixel is reclassified as snow-covered if any neighbouring pixel is snow-covered and the elevation of any snow covered pixels is higher than that of the central pixel.
- 6) Temporal interpolation. All dates before and after the given day are iteratively considered until one is found where a given pixel is not cloud-covered. Thus, each remaining cloud-covered pixel after steps 1–5 receives the value (snow-covered or snow-free) of the pixel closest in time filling in this way all the missing data.

Missing data were mainly caused by the presence of cloud cover precluding the possibility to observe the surface beneath clouds in the spectral range of visible radiation. The percentage of missing data observed is well justified considering that total cloud cover is a variable characterized over the Italian territory by a pronounced daily cycle reaching the maximum between 12UTC and 15UTC with the 1961–1990 normal values between 4.0 oktas and 4.7 oktas (Manara et al., 2023).

2.4. Calculation of snow cover metrics (duration, onset and end of snow season)

The spatial distribution and temporal evolution of snow have been studied calculating the onset of the snow season (snow onset date, SOD), duration of the snow season (snow cover duration, SCD) and the end of the snow season (snow end date, SED).

Specifically, SCD is defined as the number of days of snow cover in a hydrological year (from 1 October to 30 September):

$$SCD_{i,j} = \sum_{k=1}^n S_{i,j,k} \tag{2}$$

Where i and j are the row and column of the considered pixel, k is the day of the hydrological year, ranging between 1 and 365 or 366 for leap years and S is a binary field equal to 1 if the pixel is covered by snow and 0 if it is free from snow. Each SCD value is assigned to the year in which the January-September period falls.

Then, the onset and end of the snow cover season are defined based on the fixed-date method described by Wang and Xie (2009). Specifically, SOD is defined with respect to the sum of snow cover days between the 1st of October and the 25th of January. It is expressed as:

$$SOD_{i,j} = D - \sum_{k=1}^D S_{i,j,k} \tag{3}$$

where D is the number of days from the start of the hydrological year (1st of October equal to day 1) to the 25th of January (corresponding to day 116) and $S_{i,j,k}$ is the sum of snow covered days from 1st October to 25th January. The date 25th January was selected because it is found as the day with the highest snow cover on average in the Greater Alpine Region (Fugazza et al., 2021). Finally, SED is defined with respect to the sum of snow cover days between the 25th of January (corresponding to day 116) and the 30th of September (corresponding to day 365) as:

$$SED_{i,j} = D + \sum_{k=D}^n S_{i,j,k} \tag{4}$$

As a consequence of how the metrics are defined, they do not define the first/last day in which a pixel is covered by snow because they do not consider transient snowfall and melt-out events, which would require the definition of multiple start and end dates, or the choice of a threshold of days to filter events out. Thus, SOD and SED are more indicative of the amount of snow cover days for a given pixel in the first and last part of the hydrological year. Likewise, the snow cover duration does not imply a continuous snow cover season except at high altitudes, but it provides an indication of the number of days when a given pixel is snow covered during the hydrological year.

2.5. Analysis of variance and trends in snow cover metrics

To investigate snow cover variability in relation to geography and topography, a multilinear regression of each metric with respect to elevation, aspect, slope, latitude and longitude and a corresponding linear regression with respect to the individual variables have

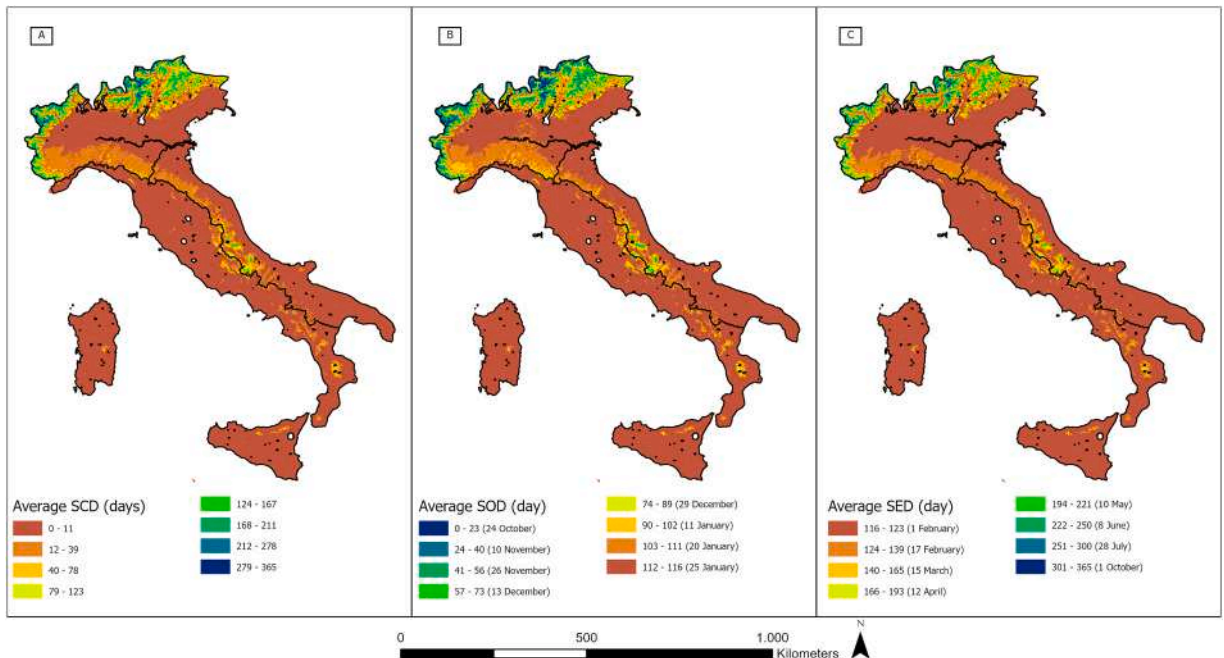


Fig. 3. (a) 2001–2022 average duration of the snow cover season (SCD) expressed in days; (b) 2001–2022 average onset of the snow cover season (SOD) expressed in days from the 1st of October (equal to 1); (c) 2001–2022 average end of the snow cover season (SED) expressed in days from the 25th of January (equal to 116).

been performed for Italy, for each region and for the different elevation bands in the different regions. To further elucidate the role of collinear variables, an ANOVA type I SS analysis was also conducted on the same set of variables over the Italian territory ordering them with different combinations in order to test their importance in describing the snow cover variability.

Then, to study the temporal evolution of the SCD series in the considered area and over the whole covered period, the SCD mean series for all the regions and the whole considered area were transformed into additive anomaly series with respect to the 2001–2022 period (i.e. difference for each year between each SCD value and the mean of the selected reference period). The trends were quantified by means of the Sen-Theil method (Sen, 1968; Theil, 1992), while the significance of the trends was evaluated by means of the Mann-Kendall non parametric test (Sneyers, 1992).

3. Results

3.1. Spatial distribution of the duration, onset and end of the snow cover season

The SCD mean values (Fig. 3a) obtained averaging the yearly SCD over the 2001–2022 period lie between 0 and 365 days. The Alps region as expected shows the highest values over the Alpine chain with a mean value equal to about 90 days for elevations above 500 m a.s.l. reaching the maximum value (365 days) where the glaciers are located. These high values depend on the fact that the number of days in which the pixels are covered by snow is often very high at high elevations, but also on the fact that MODIS does not distinguish between snow-covered and snow-free glacier areas (Fugazza et al., 2021). Well defined are the valleys showing lower values compared to the surrounding mountains, clearly reproducing the orography of the region. Conversely, the lowest values of SCD are seen over the area of the Po plain with about 5 days for elevations lower than 500 m a.s.l. However, in these areas owing to its definition SCD does often not reflect a continuous snow cover period but only the number of snow cover days in a year. In the south part of the Alps region, higher values are observed compared to the Po plain area, ranging between about 12 and 39 days owing to the presence of the northern Apennine chain. Moving to the south, the West and East Apennine regions show higher values over the Apennine chain located along the border between the two regions. The mean SCD is equal to 6 days in the West region and to 10 days in the East region. The highest values, equal to about 230 days, are seen in correspondence with the highest elevations, between 2000 and 2830 m a.s.l., located in the area of Vettore, Gran Sasso, La Maiella and La Meta mountains in the East region. Moving again to the south in the western region, the mount Pollino and La Sila are also discernible with average values of SCD equal to about 28 days and elevations between 400 and 2200 m a.s.l. Sicily and Sardinia regions show a mean SCD of 2 days and 1.9 days respectively with few grid points that reach values higher than 80 days.

The SOD (Fig. 3b) and SED (Fig. 3c) show a very similar distribution of the values to that found for SCD. In the Alps region the mean SOD and SED are day 76 (16th December) and day 166 (16th March) respectively for elevations above 500 m a.s.l. Conversely, these values are equal to day 112 (21st January) and day 119 (28th January) for lower elevations. Moving to the south the mean SOD is equal to day 113 (22nd January) in the west Apennine region and day 111 (20th January) in the east Apennine region while the mean SED is equal to day 119 (28th January) and day 122 (31st January) respectively. The lowest values of SOD and highest values of SED are found where also the highest SCD values are seen, reaching day 30 (31st October - Apennines East) and day 47 (17th November -

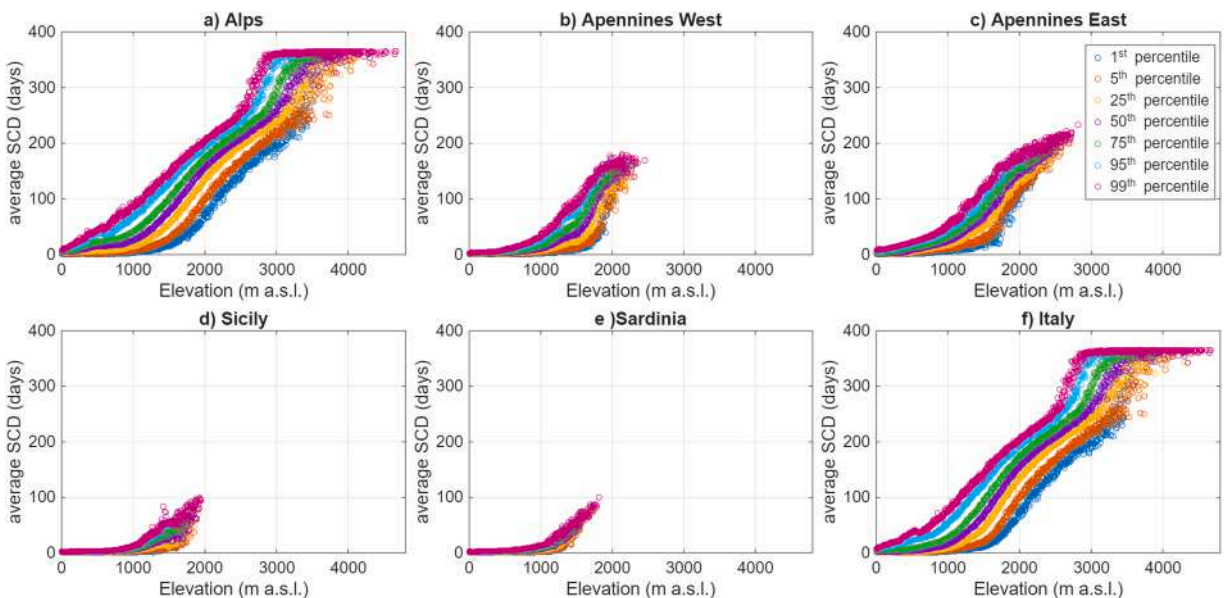


Fig. 4. Quantiles of the distribution of duration of the snow cover season (SCD) average values in the 2001–2022 period in each 5-m interval of the (a) Alps, (b) Apennines West, (c) Apennines East, (d) Sicily, (e) Sardinia and (f) Italy elevation range.

Apennines West) for SOD and day 265 (23rd June - Apennines East) and day 231 (20th May - Apennines West) for SED. Finally, the mean SOD is equal to day 115 (24th January) while SED is equal to day 117 (26th January) both in the Sicily and Sardinia region, respectively, where only very few grid-points reach values lower than day 80 (20th December) for SOD and higher than day 160 (10th March) for SED.

3.2. Factors explaining the spatial variability in the snow cover metrics

In order to investigate the dependence of SCD from the elevation, Fig. 4 shows for each region the quantiles of the distribution of average SCD in the 2001–2022 period of the pixels falling in each 5-m elevation band. For all the regions, a clear dependence of SCD from elevation is evident and as expected higher SCD values are reached where elevation is higher. Moreover, a very large spread in the SCD values is found for each elevation band and each region highlighting how the dependence of SCD from elevation is not enough to explain its variability but also the dependence from other variables should be taken into account. The range of the spread is particularly pronounced for the Alps region where the SCD values increase almost linearly with elevation until about 3000 m a.s.l. The rate of increase of SCD with elevation is almost the same for the Apennines east region even if it is less evident due to a shorter range covered by the elevations (Fig. 5). Conversely, the Apennines west region shows a lower rate of increase of SCD with elevation with a behaviour similar to that observed for Sardinia region up to about 1800 m a.s.l. In contrast, for elevations higher than 1800 m a.s.l., the rate of increase becomes more similar to that observed for the Apennines east region. Finally, Sicily shows the lowest rate of increase with elevation.

In order to better investigate the spatial distribution of the spread of the SCD values, the difference (Fig. 6) between the SCD of each pixel and the average of the SCD values for Italy falling in the corresponding 5-m elevation intervals has been calculated. The Alps region shows a complex picture with grid points featuring higher values compared to the Italian mean of the same 5-m elevation interval and grid points featuring lower values suggesting also in this case how the SCD depends not only on elevation but also on other geographical parameters (e.g., slope, aspect, longitude and latitude). As an example, the valleys are well defined with the grid points facing north having higher SCD values than the grid points facing south. The dependence on the aspect can be found in all the elevation bands lower than 4000 m a.s.l. where the highest values are found for the pixels oriented north and the lowest ones for the pixels oriented south. The difference is particularly pronounced for elevations lower than 1000 m a.s.l. where the pixels oriented south have more than 50 % fewer snow days. This percentage decreases as the elevation increases. The Po valley shows values that are in line with those obtained at the nation scale for the corresponding elevation interval even if in some regions the SCD is slightly lower (up to 5 days), especially moving to the east towards the Adriatic coast (Fig. 6). Conversely, the south part of the Po valley shows higher values (by about 5–20 days) than the corresponding Italian mean. In particular, the area of Maritime Prealps shows values that are higher by more than 20 days compared to the Italian mean. Moving to the south, the east Apennines region show values that are higher than the corresponding mean in most cases up to 20 days until the Gargano promontory. This difference decreases moving from the Apennine chain to the Adriatic coast where the SCD is slightly lower (up to 5 days) than the mean of the corresponding elevation interval as in the remaining part of the region. The same values as those found over the Adriatic coast are seen for the western Apennine region, Sicily and Sardinia that in general show lower SCD values (in most cases up to 5 days) than the mean values obtained in the corresponding elevation interval for Italy. It should be noted that the most complex situation with pixels showing large differences from the corresponding SCD mean (lower than 40 days and higher than 20 days) is found in the central part of the Apennines in correspondence with the high elevation areas of the Apennines chain. It is interesting to note how moving from north to south and especially in the south of the West Apennines region, Sicily and Sardinia the number of pixels with a lower SCD value compared to the mean of the corresponding elevation interval increases. This is in agreement with Fig. 5 that shows how for West Apennines, Sardinia and even more for Sicily the SCD values are lower than those obtained in the same elevation band in the Alps and east Apennines region.

As shown by the multilinear regression, the variance explained is about 81 %, 82 % and 78 % for the SCD, SOD and SED respectively at the Italian scale. These values are highest in the Alps, i.e. higher than 86 % for all the metrics, higher for the Apennines

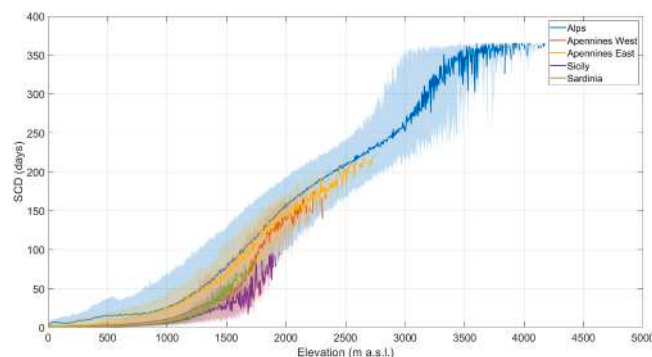


Fig. 5. Median (bold line) of the distribution of the average snow cover duration (SCD) in the 2001–2022 period in each 5-m interval for the (a) Alps (blue line); (b) Apennines West (orange line); (c) Apennines East (yellow line); (d) Sicily (violet line) and (e) Sardinia (green line). The light area represents the values lying between the 1st and 99th quantiles.

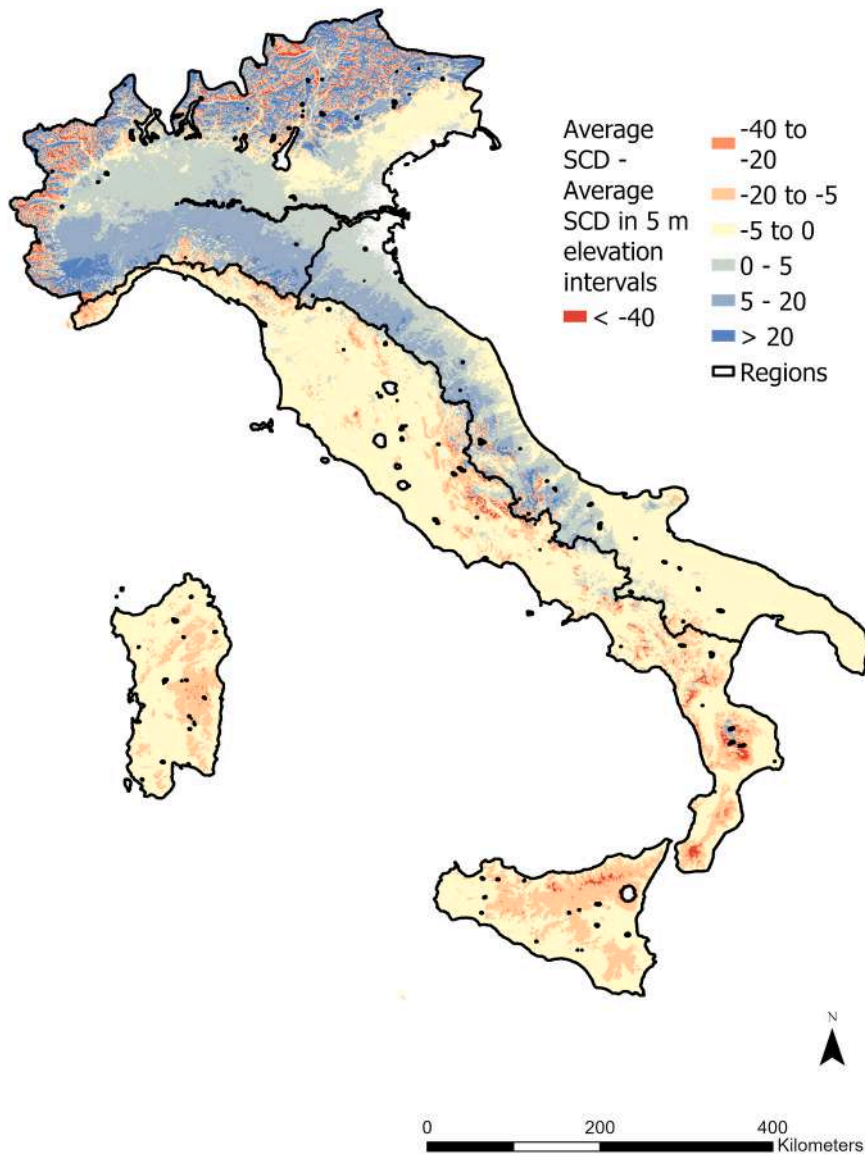


Fig. 6. Differences between the duration of the snow cover season (SCD) grid point values and the average of the Italian SCD values falling in the corresponding 5-m elevation intervals.

east than for the Apennines west (around 70 % compared to around 50 %) and lowest for Sicily and Sardinia (around 30–40 %). When the parameters are considered separately (Table 1) the most part of the variance is explained by elevation with values comparable to those observed for the multilinear regression both at the Italian and regional scale. The predominant role of elevation is evident for all regions and for all the elevation bands considering points lower than 4000 m a.s.l. (Table 2). Considering the contribution of the other parameters, slope is able to explain about 24–30 % of the variance at the Italian scale while at the regional level it has similar values only for the Alps (between 27 and 35 %) and the east Apennines (between 25 and 28 %), mostly owing to the points with elevation lower than 1000 m and higher than 4000 m a.s.l. (only for the Alps). The fraction of explained variance considering slope becomes relevant (higher than 10 %) also in the Apennines west for points between 2000 and 3000 m a.s.l. and in Sicily for points located under 1000 m a.s.l. In the other regions the explained variance is lower than 10 %. Aspect shows a fraction of explained variance different from 0 % only in the Alps region, the region with the most complex orography, higher than 4 % for points between 0 and 3000 m a.s.l., and in the elevation band between 2000 and 3000 m a.s.l. in the Apennines region. Latitude explains about 14–19 % of the variance when the whole country is considered. Values higher than 5 % are seen only in the Alps and in Sicily where probably the contribution is caused by the position of the mountains with respect to the plain area. Moreover, the contribution remains higher than 6 % for all the three metrics if points located at elevations higher than 3000 m a.s.l. are considered in the Alps and for points lower than 1000 m a.s.l. both in the Apennines East and in Sicily where the contribution increases to more than 10 %. Longitude explains about 8 % of the

Table 1

Variance explained by multilinear regression and linear regression of individual variables against the three metrics (SCD, SOD and SED) in the different sub-regions. Each cell reports the R^2 .

Region	Metric	Multilinear regression	Elevation	Aspect	Slope	Latitude	Longitude
Alps	SOD	0.89	0.86	0.02	0.35	0.18	0.01
	SED	0.86	0.82	0.01	0.27	0.14	0.01
	SCD	0.88	0.85	0.01	0.30	0.16	0.01
Apennines West	SOD	0.51	0.48	0.00	0.07	0.00	0.01
	SED	0.51	0.48	0.00	0.05	0.00	0.01
	SCD	0.52	0.49	0.00	0.06	0.00	0.01
Apennines East	SOD	0.73	0.68	0.00	0.28	0.01	0.06
	SED	0.70	0.63	0.00	0.25	0.02	0.06
	SCD	0.72	0.66	0.00	0.26	0.02	0.06
Sicily	SOD	0.42	0.41	0.00	0.08	0.10	0.00
	SED	0.37	0.36	0.00	0.05	0.05	0.00
	SCD	0.40	0.39	0.00	0.06	0.07	0.00
Sardinia	SOD	0.32	0.30	0.00	0.03	0.00	0.00
	SED	0.38	0.36	0.00	0.02	0.01	0.01
	SCD	0.36	0.35	0.00	0.02	0.01	0.00
Italy	SOD	0.82	0.76	0.00	0.30	0.19	0.09
	SED	0.78	0.73	0.00	0.24	0.14	0.07
	SCD	0.81	0.76	0.00	0.27	0.16	0.08

variance of SCE at the Italian level and 6 % in the Apennines East.

The dominant role of elevation on SCD is confirmed also by an ANOVA analysis of type I SS applied over the Italian territory. This variable explains in fact the largest fraction of variance in snow cover duration across the set of variables considered in Table 1, independently from the order of the variables in the analysis. This fraction is greater than 75 % in most cases (see Fig. 1S). The fraction of variance explained by elevation decreases to 62 % when it is introduced in the analysis after slope and aspect (Figure 1Sh) and to 55 % when it is introduced as last variable (Figure 1Sf), suggesting collinearity between elevation and some of the other variables. The rather relevant role of latitude on SCD is also confirmed by the ANOVA analysis. This variable explains between 5 % and 20 % of the variance of snow cover duration depending on the order of inclusion of the variables in the analysis (Fig. 1S). Slope explains a relevant fraction of the variance of snow cover duration only when it is considered in the analysis before elevation. Longitude has a negligible effect except when it is introduced as the first variable in the analysis, whereas the contribution of aspect is always negligible.

3.3. Interannual variability of the duration of snow cover series over the period 2001–2022

In order to investigate the interannual variability of the SCD series over the period 2001–2022 the standard deviation of the SCD for each pixel (Fig. 7a) and the corresponding ratio with respect to the 2001–2022 average (Fig. 7b) have been calculated. Overall, the standard deviation of the SCD increases as elevation increases until about 2000 m a.s.l. when it starts to decrease (Fig. 2S). In particular, moving from north to south, the Alpine chain shows a complex picture where it is possible to distinguish the valleys where lower standard deviations values are observed (Fig. 7a). The mean standard deviation observed for points located above 500 m a.s.l. in the Alps region is 15 days higher than the corresponding value obtained for points with elevation lower than 500 m a.s.l. (9 days). In fact, the Po plain shows a quite uniform behaviour with values between 0 and 10 days. Moving to the south the SCD standard deviation starts to increase approaching the Apennines chain, moving from a band that shows values of standard deviation between 10 and 15 days to an area with a more complex picture with points reaching more than 30 days. Moving to the south, the Apennines east and west show a similar behaviour with a complex picture and values generally higher than 10 days along the mountain chain and around 0–10 days elsewhere. In particular, the mean standard deviation is equal to about 5 days and 3 days if points located at elevation lower than 500 m a.s.l. are selected for the east and west Apennines respectively and 14 days and 9 days above 500 m a.s.l. Finally, the Sicily and Sardinia regions show a uniform situation with an average standard deviation equal to 3 days for both regions, with only very few points with values higher than 10 days.

Analysing the ratio between the standard deviation of the SCD series and the corresponding 2001–2022 average (Fig. 7b) shows a different pattern from the standard deviation of the SCD (Fig. 7a). In the Alps region, the orography is well reproduced showing lower values for points located at higher elevations and higher values for points located at lower elevations well delineating the different valleys. Overall, for points located at elevations higher than 500 m a.s.l. the ratio is about 0.55 while for points below 500 m a.s.l. it is about 1.36. In fact, in the Po plain a quite uniform distribution is observed with a ratio between 1 and 2.5 for most points.

With an opposite behaviour of that observed in Fig. 7a the values start to decrease moving to the south and approaching the Apennines chain. Both the Apennines west and east regions show increasing values moving from the mountain chain to the coast with a value of 0.79 and 1.12 for points above 500 m a.s.l. in the east and west region respectively and 1.70 and 1.73 for points below 500 m a.s.l. Interestingly, the pattern observed in the east Apennines region is more similar to that observed in the Alps region until the Gargano promontory while south of the Gargano promontory the ratio shows a similar behaviour to that observed for the west Apennines region, Sicily and Sardinia. In fact, most points south of the Gargano promontory have a ratio higher than 1.50 as in Sicily and Sardinia region where the mean value is about 1.92 and 1.78, respectively. In order to explain the variability of the ratio of the standard deviation of the SCD in the 2001–2022 period over the corresponding mean the quantile distribution of the ratio in every 5-m

Table 2Variance explained by linear regression of individual variables against the three metrics (SCD, SOD and SED) in the different sub-regions and elevation bands. Each cell reports the R².

		0-1000			1000-2000			2000-3000			3000-4000			> 4000		
		SOD	SED	SCD	SOD	SED	SCD	SOD	SED	SCD	SOD	SED	SCD	SOD	SED	SCD
Alps	Elevation	0.34	0.37	0.38	0.56	0.60	0.61	0.51	0.53	0.54	0.18	0.26	0.25	0.00	0.02	0.02
	Aspect	0.10	0.08	0.10	0.11	0.04	0.07	0.10	0.06	0.07	0.02	0.01	0.01	0.00	0.00	0.00
	Slope	0.17	0.10	0.14	0.01	0.00	0.00	0.02	0.03	0.03	0.00	0.00	0.00	0.15	0.14	0.14
	Latitude	0.00	0.08	0.02	0.06	0.02	0.04	0.01	0.01	0.01	0.14	0.07	0.08	0.06	0.08	0.08
	Longitude	0.02	0.06	0.04	0.00	0.00	0.00	0.00	0.00	0.00	0.09	0.03	0.04	0.09	0.10	0.10
Apennines West	Elevation	0.34	0.48	0.46	0.54	0.55	0.56	0.14	0.15	0.16						
	Aspect	0.00	0.00	0.00	0.00	0.00	0.00	0.04	0.11	0.09						
	Slope	0.07	0.04	0.06	0.00	0.00	0.00	0.13	0.17	0.17						
	Latitude	0.00	0.00	0.00	0.05	0.03	0.04	0.05	0.00	0.01						
	Longitude	0.01	0.01	0.01	0.02	0.01	0.01	0.00	0.02	0.01						
Apennines East	Elevation	0.57	0.51	0.56	0.68	0.72	0.72	0.55	0.61	0.60						
	Aspect	0.00	0.00	0.00	0.00	0.00	0.00	0.06	0.04	0.05						
	Slope	0.30	0.30	0.31	0.03	0.01	0.02	0.01	0.02	0.01						
	Latitude	0.13	0.22	0.18	0.01	0.00	0.00	0.01	0.00	0.00						
	Longitude	0.23	0.33	0.29	0.01	0.00	0.00	0.02	0.04	0.03						
Sicily	Elevation	0.31	0.35	0.40	0.55	0.60	0.59									
	Aspect	0.01	0.01	0.01	0.00	0.00	0.00									
	Slope	0.15	0.09	0.14	0.00	0.00	0.00									
	Latitude	0.24	0.10	0.20	0.04	0.04	0.04									
	Longitude	0.01	0.01	0.01	0.00	0.00	0.00									
Sardinia	Elevation	0.29	0.41	0.42	0.78	0.78	0.79									
	Aspect	0.00	0.00	0.00	0.00	0.00	0.00									
	Slope	0.01	0.01	0.01	0.04	0.03	0.03									
	Latitude	0.02	0.04	0.04	0.01	0.00	0.00									
	Longitude	0.02	0.00	0.00	0.00	0.00	0.00									

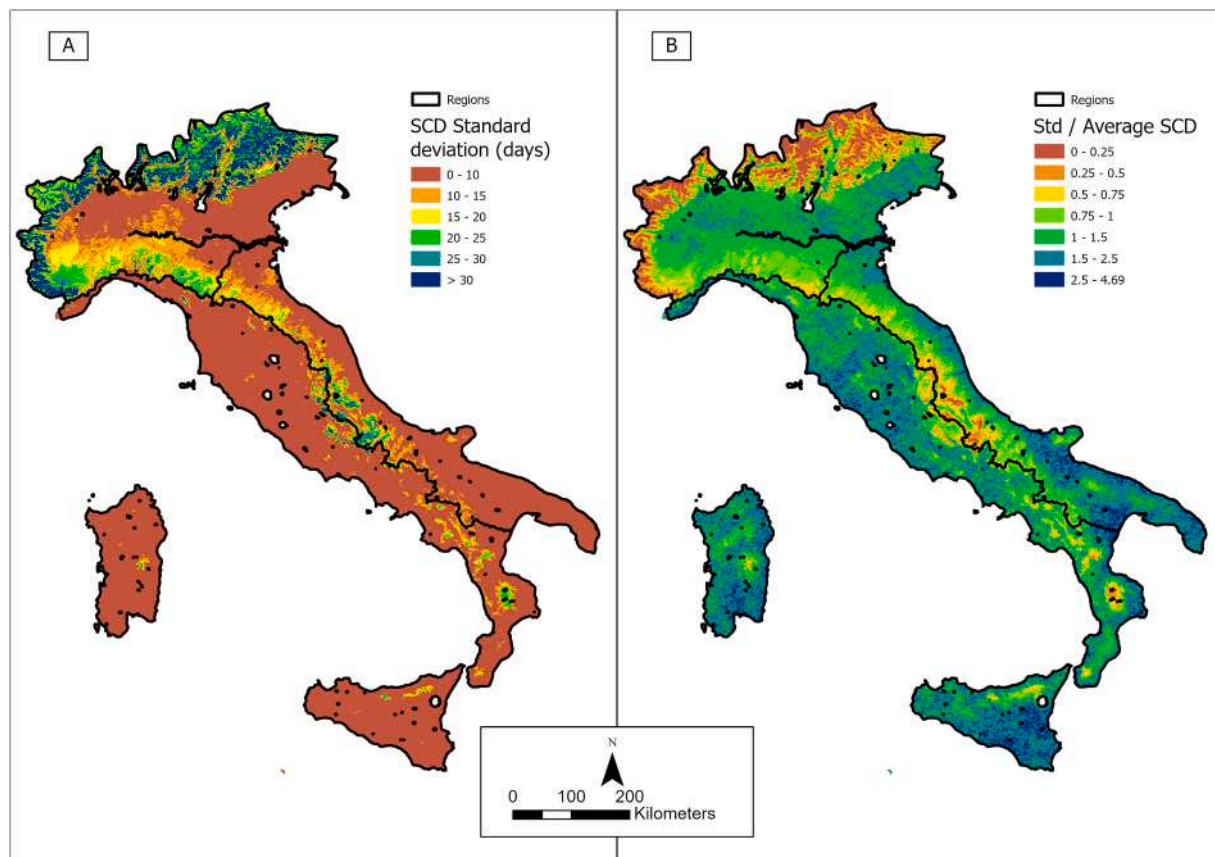


Fig. 7. (a) Standard deviation of the duration of the snow cover season (SCD) series calculated over the 2001–2022 period expressed in days; (b) Ratio between the standard deviation of the SCD and the corresponding mean calculated over the 2001–2022 period.

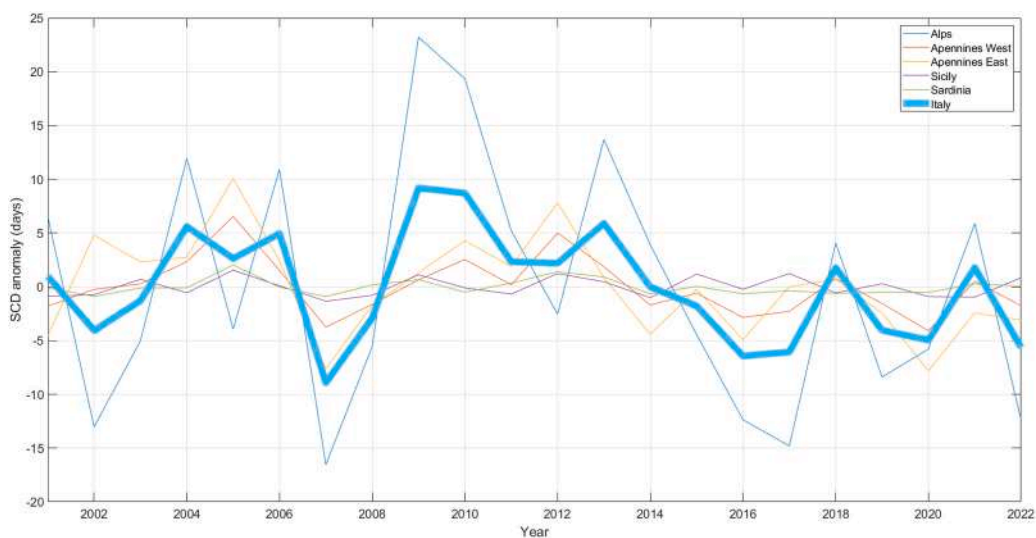


Fig. 8. Temporal evolution of the additive anomaly series of the average duration of the snow cover season (SCD) series in the period 2001–2022. The bold line is the Italian mean series while the thin lines are the regional mean series.

elevation interval (Fig. 3S) has been plotted. In all the regions, the ratio decreases as elevation increases and as expected the range of the ratio is lower for the regions where higher SCD values (Figs. 3 and 4) and lower SCD standard deviation (Fig. 7a) are observed.

3.4. Trend analysis of the duration of the snow cover series over the 2001-2022 period

Analysing the additive anomaly series over Italian regions (see Fig. 8), the Apennines east is the only region where the series shows a significant trend, equal to -3.2 days per decade ($p < 0.05$). If specific elevation bands are considered (Figs. 4S, 9), the SCD series at Italian scale shows a significant negative trend at elevations higher than 3500 m a.s.l. due to the signal observed over the Alps. The decrease for both the Italian and Alps regions is between -5.1 days per decade and -0.6 days per decade ($p < 0.1$) depending on the selected elevation band. Similarly, for elevations higher than 3000 m a.s.l., the SED shows a significant negative trend at the Italian scale and in the Alps between -5.7 days per decade and -0.5 days per decade ($p < 0.1$). Conversely, the SOD shows a significant positive trend in the elevation band between 4000 and 4500 m a.s.l. of about 0.2–0.3 days per decade ($p < 0.05$).

For elevations lower than 3500 m a.s.l. the trend is negative and significant ($p < 0.05$) only in the Apennines region (between 500 m a.s.l. and 1500 m a.s.l.) with values between -6.2 and -9.9 days per decade. The SOD series are not significant in any region and elevation band while the SED shows a significant negative trend of about -8.0 days per decade ($p < 0.1$) only for elevations between 1500 m and 2000 m a.s.l. in the Apennines west region. In Sicily and Sardinia, the trends for all the elevation bands and all the three metrics are not significant.

Investigating the spatial distribution of the SCD trends (Fig. 10) it is possible to observe that most of the pixels show a negative value. The most negative values are observed over the Alpine and Apennines chain reaching values lower than -15 days per decade. Only very few pixels located in the eastern part of the Alpine chain show positive values even if in most cases not significant.

4. Discussion

4.1. Spatial distribution of snow cover metrics

The spatial distribution of the investigated snow cover duration metrics over the 2001–2022 period shows a complex picture (Sections 3.1 and 3.2). As expected, the SCD strongly depends on elevation even if the large spread in the SCD values found for each elevation band highlights how also the dependence from other variables (i.e., slope, aspect, latitude, longitude) should be taken into account. In particular, the variance explained by the multilinear regression with respect to elevation, aspect, slope, latitude and longitude, exceeds 86 % for all the metrics in the Alps region. In the Apennines, the explained variance is higher in the eastern sector than in the western one (around 70 % compared to approximately 50 %), and it is lowest in Sicily and Sardinia (around 30–40 %). Beside the role of elevation, slope can explain 24–30 % of the variance at the Italian scale. Finally, considering the large extension of the Italian territory, latitude explains about 14–19 % of the variance. Comparable results are obtained applying an ANOVA analysis of type I SS to the snow cover fields of the entire Italian territory, highlighting again the dominant role of elevation. Slope and latitude show a relevant contribution only when they are considered in the analysis before elevation while longitude has a negligible effect except when it is considered as the first variable in the analysis. Finally, the contribution of aspect is always negligible.

The most remarkable geographic effect influencing snow cover duration in the peninsular part of Italy is the difference observed between the Eastern and the Western part of the Apennine chain. It is due to the orientation (NW-SE) of this chain, which causes a greater impact on the north-eastern slopes of the cold air masses coming from the Balkan region and eastern Europe. These air masses can induce abundant snowfall through the vertical transport of moisture and heat connected to their passage over the Adriatic Sea and

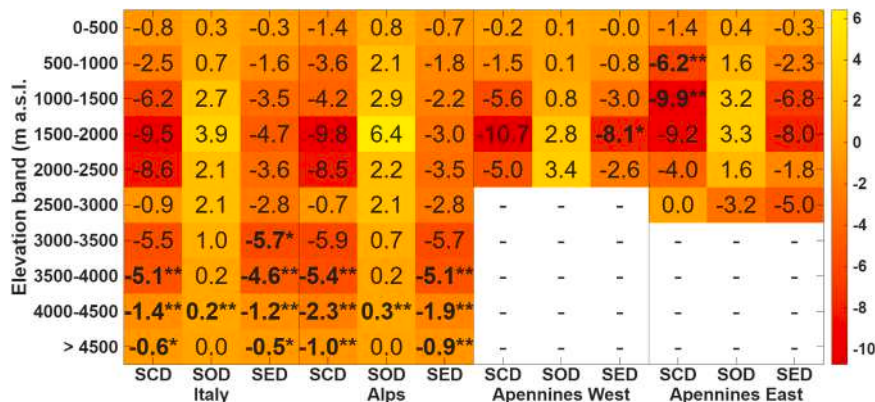


Fig. 9. Trends expressed as days per decade over the periods 2001–2022 for Italy, Alps, Apennines east and west regions, for snow cover duration (SCD), snow cover onset (SOD) and snow cover end (SED). Cells are color-coded based on trend intensity. Values are shown in bold with one asterisk for $0.05 < p < 0.1$ and in bold with two asterisks for $p < 0.05$. The trends are estimated with the Theil-Sen method, while the significance of the trends is evaluated with the Mann-Kendall non-parametric test.

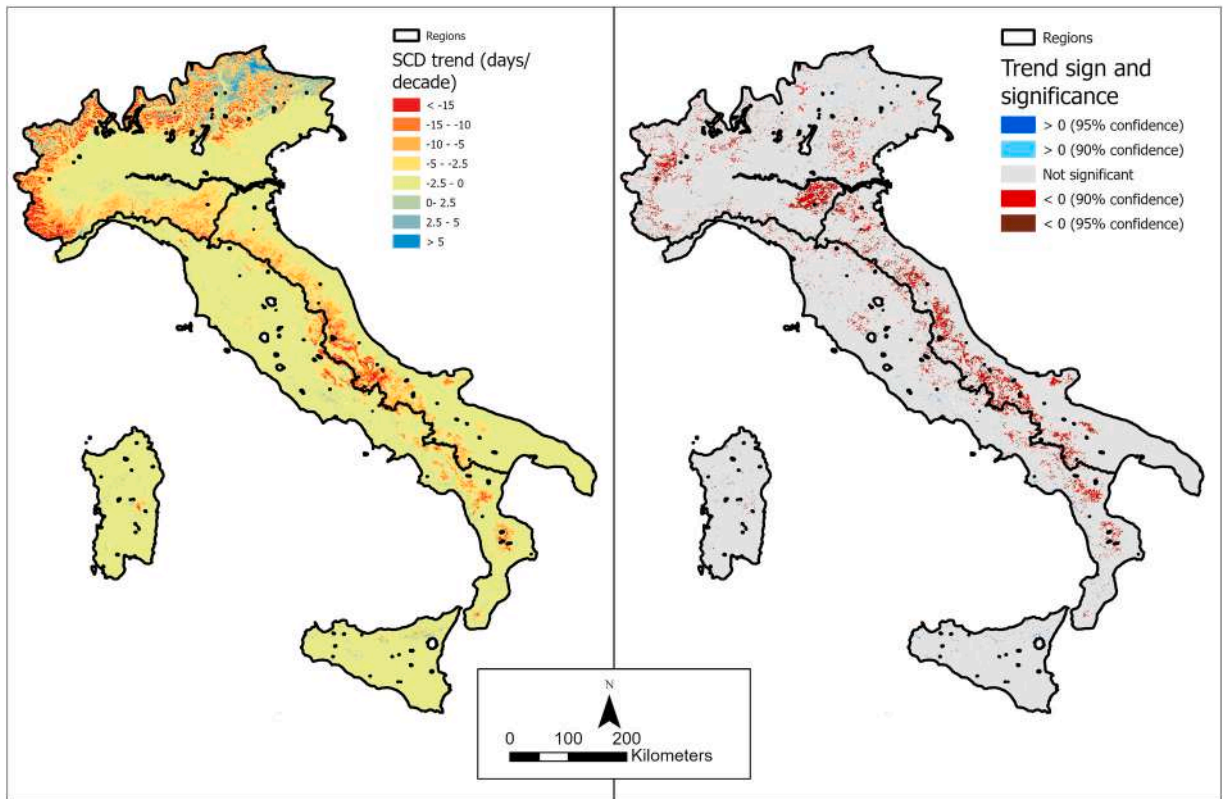


Fig. 10. (a) Spatial distribution of the SCD trends over the 2001–2022 period expressed in days per decade; (b) Spatial distribution of the pixels that report a significant trend evaluated with the Mann-Kendall non parametric test. Negative trends are represented with light blue for $0.05 < p < 0.1$ and dark blue for $p < 0.05$. Positive trends are represented with light red for $0.05 < p < 0.1$ and dark red for $p < 0.05$.

the orographic forcing, which is related to their interaction with the mountain range (Capozzi et al., 2025).

4.2. Interannual variability and temporal trends in snow cover metrics

The temporal evolution of the investigated snow cover duration metrics over the 2001–2022 period shows a very high interannual variability resulting in a negative trend that however in most cases is not significant (Section 3.3 and Section 3.4).

In order to investigate more in depth the temporal evolution of the SCD series, the mean relative anomaly series with respect to the 2001–2022 period was calculated for each sub-region and compared with the corresponding series of the Snow Cover Extent (SCE) obtained from ERA5-Land (Fig. 5S). In particular, the anomaly series is here calculated as the ratio with respect to the 2001–2022 period unlike in Fig. 8 where it is calculated as the difference, in order to make it comparable with that obtained with SCE.

The agreement between the MODIS SCD and ERA5-Land SCE series is very good, resulting in a correlation of about 0.91 at the Italian scale and always higher than 0.97 if the sub-regions are considered. The trends for both are negative for all the sub-regions even if they are significant ($p < 0.05$) only for the Apennines East region where they are about -30% per decade.

Considering the good agreement between the MODIS SCD series and the ERA5-Land SCE series, the temporal evolution of SCE over the whole available period of ERA5-Land (1951–2022) has been evaluated (Fig. 11). Specifically, the SCE relative anomaly series, with respect to the 2001–2022 period, shows a significant decreasing trend of about 4% per decade over the Italian territory, corresponding to about 28% over the investigated period, especially due to the signal observed over the Alps. In fact, the other sub-regions do not show a significant trend. This situation is found also if subperiods of the whole period are considered. The Italian territory and the Alps region show significant trends for windows starting before 1980, while the other sub-regions show only very few significant windows (Fig. 6S).

4.3. Snow cover changes in Italy and links to climate evolution

The results of this study are in agreement with those reported in literature even if they depend on the period, considered area, elevation and time of aggregation, making it difficult to delineate an overall picture. For example, Annella et al. (2023) found at Montevergine Observatory (1280 m a.s.l.) in the Apennines an overall decrease of in-situ snow cover duration over the period 1931–2008, most notable in the winter season, until the mid of 1990s and then a rebound in the last period, as well as strong decadal

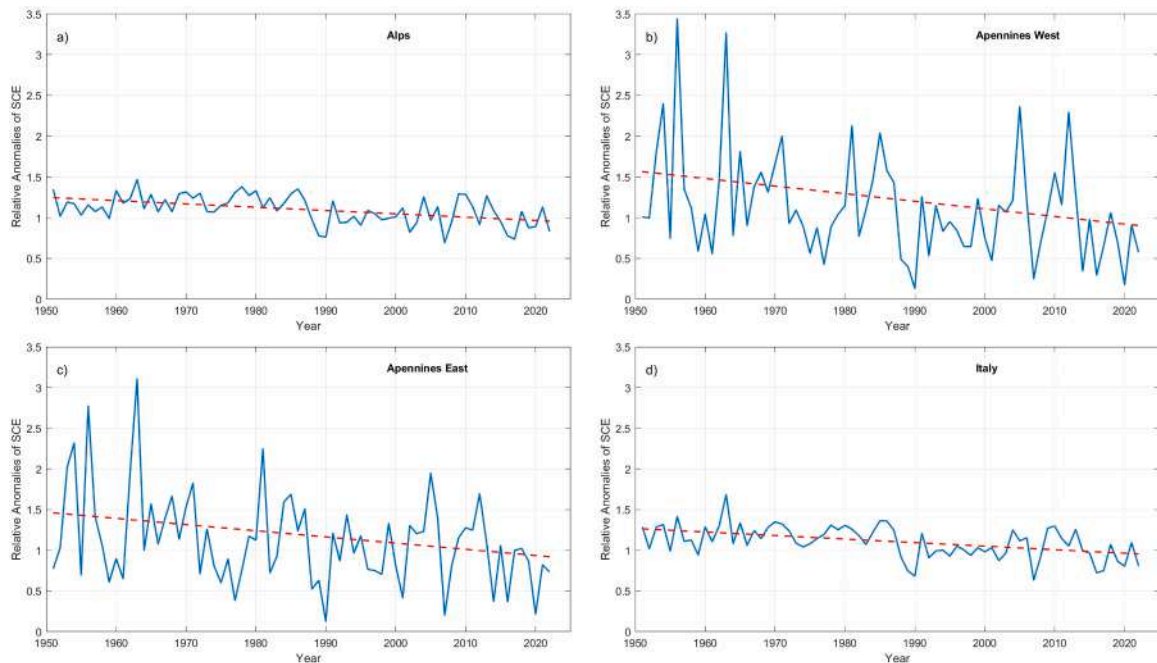


Fig. 11. SCE relative anomaly series for (a) Alps, (b) West Apennines, (c) East Apennines and (d) Italy with respect to the 2001–2022 period together with the corresponding linear regression (dashed red line).

and interannual variabilities. They ascribed the observed trends to the gradual increase in air temperature. Similarly, [Capozzi et al. \(2025\)](#) found a decreasing trend in snow cover duration over the 1951–2001 period in Central and Southern Apennines, strongly dependent on elevation.

In parallel, long-term analyses over the Alps region identified periods of high snow cover in the 1940s/50 s, as well as in the 1960s/70 s, followed by absolute minima in the 1980s and early 1990s with some recovery afterwards ([Matiu et al., 2021](#); [Terzago et al., 2010](#); [Valt and Cianfarrà, 2010](#)). Moreover, over the same domain and over the 1920–2020 period, [Bozzoli et al. \(2024\)](#) found that the observed decreasing trend in snowfall is also dependent on elevation reporting a larger negative trend for stations at lower altitudes than those at higher altitudes.

The analysis performed in this study helps increase the knowledge of the spatial distribution and temporal evolution of the duration of the snow cover season over the Italian Alps and Apennines chain. The results also improve our understanding of the climate evolution over the Italian territory where precipitation showed a stationary pattern over the last decades ([Chimani et al., 2023](#); [Vicente-Serrano et al., 2025](#)), while air temperature has experienced a strong increase especially due to the signal observed after the 1980s. In parallel, surface solar radiation ([Manara et al., 2016, 2019a, 2020](#)) which is directly related to snow cover and influences its extent, showed a decrease until the mid of the 1980s (global dimming) and a subsequent increase (brightening period), owing to a combination of the total cloud cover decrease observed until the 1990s ([Manara et al., 2023](#)) and an increase of aerosol concentration observed until the mid-1980s and a subsequent reversing signal ([Manara et al., 2019b](#)). Further studies will be necessary to extend the results presented in this study. For example, it will be interesting to compare the results with those obtained from other high-resolution reanalysis products (both for the spatial distribution and temporal evolution) or to extend into the past the satellite series presented here with those available from other satellite sources (e.g. AVHRR). Moreover, it will be interesting to validate the MODIS data with ground station data from the same period.

5. Conclusion

In Italy, snow cover is an important socioeconomic resource for the agriculture, tourism and industry sector. It includes the Alps region but also the Apennine chain where a detailed knowledge of snow cover is even more important, as the snow resource is mostly unexploited, and the region is affected by frequent drought episodes. In this context, in this study, the distribution of snow cover variables and their temporal evolution is analysed over the whole Italian territory, between 2000 and 2022, using MODIS data acquired from the Terra and Aqua platforms and then compared with the SCE data obtained using reanalysis datasets such as ECMWF-ERA5 Land data. In particular, after a pre-processing of data in order to fill missing data ([Section 2.3](#)) and to obtain for each pixel a binary field (snow or snow free), the onset (SOD), the duration (SCD) and the end (SED) of the snow season have been calculated ([Section 2.4](#)) and analysed.

The spatial distribution of the obtained metrics ([Section 3.1](#)) shows a complex picture with the highest values observed for the higher elevations (i.e. Alps and Apennines chain). However, a very large spread in the SCD values is found for each elevation

highlighting how even though elevation is the factor explaining the most part of the snow cover spatial variability, it should be considered together with the effect of the other geographical parameters (e.g., slope, aspect, longitude, latitude).

Besides the spatial distribution of SCD, SOD and SED also their interannual variability and temporal evolution have been investigated (Section 3.3) over the whole considered period, highlighting how, due to the observed high interannual variability, the resulting trend even if negative in most cases is not significant. The good agreement found between the temporal evolution of SCD and the snow cover extent (SCE) obtained from ERA5-Land allowed to evaluate the trend starting from the 1950s, which was found significant over the Italian territory mainly due to the signal observed over the Alps region.

The consistency of this trend could be further explored, through a comparison with other datasets from reanalysis and satellite sources (e.g. AVHRR), as well as ground station data from the same period, to obtain a comprehensive picture of snow cover variations of the Italian territory.

CRedit authorship contribution statement

Veronica Manara: Writing – review & editing, Writing – original draft, Software, Methodology, Investigation, Formal analysis, Data curation, Conceptualization. **Guglielmina Adele Diolaiuti:** Writing – review & editing, Supervision, Conceptualization. **Cecilia Delia Almagioni:** Writing – review & editing, Software, Methodology, Investigation, Formal analysis, Data curation, Conceptualization. **Davide Fugazza:** Writing – review & editing, Writing – original draft, Software, Methodology, Investigation, Formal analysis, Data curation, Conceptualization. **Maurizio Maugeri:** Writing – review & editing, Supervision, Project administration, Methodology, Funding acquisition, Formal analysis, Conceptualization.

Declaration of Competing Interest

The authors declare that they have no known competing financial interests or personal relationships that could have appeared to influence the work reported in this paper.

Acknowledgements/Funding

This work has been funded by Research Funds from the Italian Ministry for University and Research (PRIN 2022-CN4RWK-CCHP-ALPS-Climate Change and HydroPower in the Alps, funded by the European Union (Programme Next Generation EU)). Veronica Manara was supported by the “Ministero dell’Università e della Ricerca” of Italy [grant FSE-REACT EU, DM 10/08/2021 n. 1062].

Appendix A. Supporting information

Supplementary data associated with this article can be found in the online version at [doi:10.1016/j.ejrh.2025.102895](https://doi.org/10.1016/j.ejrh.2025.102895).

Data availability

Data used are available from public sources.

References

- Almagioni, C.D., Manara, V., Diolaiuti, G.A., Maugeri, M., Spezza, A., Fugazza, D., 2025. Snow cover variability and trends over Karakoram, Western Himalaya and Kunlun Mountains during the MODIS era (2001–2024). *Remote Sens.* 17, 914. <https://doi.org/10.3390/rs17050914>.
- Annella, C., Budillon, G., Capozzi, V., 2023. On the role of local and large-scale atmospheric variability in snow cover duration: a case study of Montevergine observatory (Southern Italy). *Environ. Res. Commun.* 5, 031005. <https://doi.org/10.1088/2515-7620/acc3e3>.
- Bormann, K.J., Brown, R.D., Derksen, C., Painter, T.H., 2018. Estimating snow-cover trends from space. *Nat. Clim. Change* 8, 924–928. <https://doi.org/10.1038/s41558-018-0318-3>.
- Bozzoli, M., Crespi, A., Matiu, M., Majone, B., Giovannini, L., Zardi, D., Brugnara, Y., Bozzo, A., Berro, D.C., Mercalli, L., Bertoldi, G., 2024. Long-term snowfall trends and variability in the Alps. *Int. J. Climatol.* 44, 4571–4591. <https://doi.org/10.1002/joc.8597>.
- Brown, R.D., Smith, C., Derksen, C., Mudryk, L., 2021. Canadian in situ snow cover trends for 1955–2017 including an assessment of the impact of automation. *Atmosphere Ocean* 59, 77–92. <https://doi.org/10.1080/07055900.2021.1911781>.
- Buttafuoco, G., Caloiero, T., 2014. Drought events at different timescales in southern Italy (Calabria). *J. Maps* 10, 529–537. <https://doi.org/10.1080/17445647.2014.891267>.
- Capozzi, V., Serrapica, F., Rocco, A., Annella, C., Budillon, G., 2025. Historical snow measurements in the central and southern Apennine Mountains: climatology, variability, and trend. *Cryosphere* 19, 565–595. <https://doi.org/10.5194/tc-19-565-2025>.
- Chimani, B., Bochníček, O., Brunetti, M., Ganekind, M., Holec, J., Izsák, B., Lakatos, M., Tadić, M.P., Manara, V., Maugeri, M., Šfajstný, P., Szentes, O., Zardi, D., 2023. Revisiting HISTALP precipitation dataset. *Int. J. Climatol.* 43, 7381–7411. <https://doi.org/10.1002/joc.8270>.
- Colombo, N., Guyennon, N., Valt, M., Salerno, F., Godone, D., Cianfarra, P., Freppaz, M., Maugeri, M., Manara, V., Acquaootta, F., Petrangeli, A.B., Romano, E., 2023. Unprecedented snow-drought conditions in the Italian Alps during the early 2020s. *Environ. Res. Lett.* 18, 074014. <https://doi.org/10.1088/1748-9326/acdb88>.
- D’Agata, C., Bocchiola, D., Soncini, A., Maragno, D., Smiraglia, C., Diolaiuti, G.A., 2018. Recent area and volume loss of Alpine glaciers in the Adda River of Italy and their contribution to hydropower production. *Cold Reg. Sci. Technol.* 148, 172–184. <https://doi.org/10.1016/j.coldregions.2017.12.010>.
- Deshpande, P., Lehtikoinen, P., Thorogood, R., Lehtikoinen, A., 2022. Snow depth drives habitat selection by overwintering birds in built-up areas, farmlands and forests. *J. Biogeogr.* 49, 630–639. <https://doi.org/10.1111/jbi.14326>.

- Dietz, A.J., Wohner, C., Kuenzer, C., 2012. European snow cover characteristics between 2000 and 2011 derived from improved MODIS daily snow cover products. *Remote Sens.* 4, 2432–2454. <https://doi.org/10.3390/rs4082432>.
- Diodato, N., Bertolin, C., Bellocchi, G., 2020. Multi-decadal variability in the snow-cover reconstruction at parma observatory (Northern Italy, 1681–2018 CE). *Front. Earth Sci.* 8. <https://doi.org/10.3389/feart.2020.561148>.
- Engelhardt, M., Schuler, T.V., Andreassen, L.M., 2014. Contribution of snow and glacier melt to discharge for highly glacierised catchments in Norway. *Hydrol. Earth Syst. Sci.* 18, 511–523. <https://doi.org/10.5194/hess-18-511-2014>.
- Estilow, T.W., Young, A.H., Robinson, D.A., 2015. A long-term Northern Hemisphere snow cover extent data record for climate studies and monitoring. *Earth Syst. Sci. Data* 7, 137–142. <https://doi.org/10.5194/essd-7-137-2015>.
- Flanner, M.G., Shell, K.M., Barlage, M., Perovich, D.K., Tschudi, M.A., 2011. Radiative forcing and albedo feedback from the Northern Hemisphere cryosphere between 1979 and 2008. *Nat. Geosci.* 4, 151–155. <https://doi.org/10.1038/ngeo1062>.
- Fugazza, D., Manara, V., Senese, A., Diolaiuti, G., Maugeri, M., 2021. Snow cover variability in the Greater Alpine region in the MODIS era (2000–2019). *Remote Sens.* 13, 2945. <https://doi.org/10.3390/rs13152945>.
- Fugazza, D., Shaw, T.E., Mashtayeva, S., Brock, B., 2020. Inter-annual variability in snow cover depletion patterns and atmospheric circulation indices in the Upper Irtysh basin, Central Asia. *Hydrol. Process.* 34, 3738–3757. <https://doi.org/10.1002/hyp.13843>.
- Gafurov, A., Bárdossy, A., 2009. Cloud removal methodology from MODIS snow cover product. *Hydrol. Earth Syst. Sci.* 13, 1361–1373. <https://doi.org/10.5194/hess-13-1361-2009>.
- Gazzolo, M., Pinna, S., 1973. La nevosità in Italia nel quarantennio 1921-1960: gelo, neve e manto nevoso. *Ist. Poligr. dello Stato*.
- Gilbert, S.L., Hundertmark, K.J., Person, D.K., Lindberg, M.S., Boyce, M.S., 2017. Behavioral plasticity in a variable environment: snow depth and habitat interactions drive deer movement in winter. *J. Mammal.* 98, 246–259.
- Godone, D., Garnero, G., Filippa, G., Freppaz, M., Terzago, S., Rivella, E., Salandini, A., Barbero, S., 2011. Snow cover extent and duration in MODIS time series: A comparison with in-situ measurements (Provincia Verbano Cusio Ossola, NW Italy). Proceedings of the 2011 International Conference on Multimedia Technology. Presented at the 2011 International Conference on Multimedia Technology, pp. 4092–4095. <https://doi.org/10.1109/ICMT.2011.6002893>.
- Hall, D.K., Riggs, G.A., 2021a. MODIS/Terra Snow Cover Daily L3 Global 500m SIN Grid, Version 61. (<https://doi.org/10.5067/MODIS/MOD10A1.061>).
- Hall, D.K., Riggs, G.A., 2021b. MODIS/Aqua Snow Cover Daily L3 Global 500m Grid, Version 61. (<https://doi.org/10.5067/MODIS/MYD10A1.061>).
- Hersbach, H., Bell, B., Berrisford, P., Hirahara, S., Horányi, A., Muñoz-Sabater, J., Nicolas, J., Peubey, C., Radu, R., Schepers, D., Simmons, A., Soci, C., Abdalla, S., Abellan, X., Balsamo, G., Bechtold, P., Biavati, G., Bidlot, J., Bonavita, M., Chiara, G.D., Dahlgren, P., Dee, D., Diamantakis, M., Dragani, R., Flemming, J., Forbes, R., Fuentes, M., Geer, A., Haimberger, L., Healy, S., Hogan, R.J., Hólm, E., Janisková, M., Keeley, S., Lalouaux, P., Lopez, P., Lupu, C., Radnoti, G., Rosnay, P., Rozum, I., Vamborg, F., Villaume, S., Thépaut, J.-N., 2020. The ERA5 global reanalysis. *Q. J. R. Meteorol. Soc.* 146, 1999–2049. <https://doi.org/10.1002/qj.3803>.
- Hüsler, F., Jonas, T., Riffler, M., Musial, J.P., Wunderle, S., 2014. A satellite-based snow cover climatology (1985–2011) for the European Alps derived from AVHRR data. *Cryosphere* 8, 73–90. <https://doi.org/10.5194/tc-8-73-2014>.
- Keller, F., Goyette, S., Beniston, M., 2005. Sensitivity analysis of snow cover to climate change scenarios and their impact on plant habitats in Alpine Terrain. *Clim. Change* 72, 299–319. <https://doi.org/10.1007/s10584-005-5360-2>.
- Kouki, K., Luojus, K., Riihelä, A., 2023. Evaluation of snow cover properties in ERA5 and ERA5-Land with several satellite-based datasets in the Northern Hemisphere in spring 1982–2018. *Cryosphere* 17, 5007–5026. <https://doi.org/10.5194/tc-17-5007-2023>.
- Kunkel, K.E., Robinson, D.A., Champion, S., Yin, X., Estilow, T., Frankson, R.M., 2016. Trends and extremes in Northern Hemisphere Snow Characteristics. *Curr. Clim. Change Rep.* 2, 65–73. <https://doi.org/10.1007/s40641-016-0036-8>.
- Manara, V., Bassi, M., Brunetti, M., Cagnazzi, B., Maugeri, M., 2019a. 1990–2016 surface solar radiation variability and trend over the Piedmont region (Northwest Italy). *Theor. Appl. Climatol.* 136, 849–862. <https://doi.org/10.1007/s00704-018-2521-6>.
- Manara, V., Brunetti, M., Celozzi, A., Maugeri, M., Sanchez-Lorenzo, A., Wild, M., 2016. Detection of dimming/brightening in Italy from homogenized all-sky and clear-sky surface solar radiation records and underlying causes (1959–2013). *Atmos. Chem. Phys.* 16, 11145–11161. <https://doi.org/10.5194/acp-16-11145-2016>.
- Manara, V., Brunetti, M., Gilardoni, S., Landi, T.C., Maugeri, M., 2019b. 1951–2017 changes in the frequency of days with visibility higher than 10 km and 20 km in Italy. *Atmos. Environ.* 214, 116861. <https://doi.org/10.1016/j.atmosenv.2019.116861>.
- Manara, V., Brunetti, M., Wild, M., Maugeri, M., 2023. Variability and trends of the total cloud cover over Italy (1951–2018). *Atmos. Res.* 285, 106625. <https://doi.org/10.1016/j.atmosres.2023.106625>.
- Manara, V., Stocco, E., Brunetti, M., Diolaiuti, G.A., Fugazza, D., Pfeifroth, U., Senese, A., Trentmann, J., Maugeri, M., 2020. Comparison of Surface Solar Irradiance from Ground Observations and Satellite Data (1990–2016) over a Complex Orography Region (Piedmont—Northwest Italy). *Remote Sens.* 12, 3882. <https://doi.org/10.3390/rs12233882>.
- Mankin, J.S., Viviroli, D., Singh, D., Hoekstra, A.Y., Duffenbaugh, N.S., 2015. The potential for snow to supply human water demand in the present and future. *Environ. Res. Lett.* 10, 114016. <https://doi.org/10.1088/1748-9326/10/11/114016>.
- Matiu, M., Crespi, A., Bertoldi, G., Carmagnola, C.M., Marty, C., Morin, S., Schöner, W., Cat Berro, D., Chiogna, G., De Gregorio, L., Kotlarski, S., Majone, B., Resch, G., Terzago, S., Valt, M., Beozzo, W., Cianfarra, P., Gouttevin, I., Marcolini, G., Notarnicola, C., Pettita, M., Scherrer, S.C., Strasser, U., Winkler, M., Zebisch, M., Ciogna, A., Cremonini, R., Debernardi, A., Faletto, M., Gaddo, M., Giovannini, L., Mercalli, L., Soubeyroux, J.-M., Sušnik, A., Trenti, A., Urbani, S., Weigluni, V., 2021. Observed snow depth trends in the European Alps: 1971–2019. *Cryosphere* 15, 1343–1382. <https://doi.org/10.5194/tc-15-1343-2021>.
- Moreno-Gené, J., Sánchez-Pulido, L., Cristóbal-Fransi, E., Daries, N., 2018. The economic sustainability of snow tourism: the case of Ski Resorts in Austria, France, and Italy. *Sustainability* 10, 3012. <https://doi.org/10.3390/su10093012>.
- Mudryk, L., Santolaria-Otin, M., Krinner, G., Ménégot, M., Derksen, C., Brutel-Vuilmet, C., Brady, M., Essery, R., 2020. Historical Northern Hemisphere snow cover trends and projected changes in the CMIP6 multi-model ensemble. *Cryosphere* 14, 2495–2514. <https://doi.org/10.5194/tc-14-2495-2020>.
- Muñoz-Sabater, J., Dutra, E., Agustí-Panareda, A., Albergel, C., Arduini, G., Balsamo, G., Boussetta, S., Chouga, M., Harrigan, S., Hersbach, H., Martens, B., Miralles, D.G., Piles, M., Rodríguez-Fernández, N.J., Zsoter, E., Buontempo, C., Thépaut, J.-N., 2021. ERA5-land: a state-of-the-art global reanalysis dataset for land applications. *Earth Syst. Sci. Data* 13, 4349–4383. <https://doi.org/10.5194/essd-13-4349-2021>.
- Pascale, S., Ragone, F., 2025. Widespread multi-year droughts in Italy: identification and causes of development. *Int. J. Climatol.* 45, e8827. <https://doi.org/10.1002/joc.8827>.
- Rixen, C., Teich, M., Lardelli, C., Gallati, D., Pohl, M., Pütz, M., Bebi, P., 2011. Winter tourism and climate change in the Alps: an assessment of resource consumption, snow reliability, and future snowmaking potential. *Mt. Res. Dev.* 31, 229–236.
- Salomonson, V.V., Appel, I., 2006. Development of the Aqua MODIS NDSI fractional snow cover algorithm and validation results. *IEEE Trans. Geosci. Remote Sens.* 44, 1747–1756. <https://doi.org/10.1109/TGRS.2006.876029>.
- Sen, P.K., 1968. Estimates of the regression coefficient based on Kendall's Tau. *J. Am. Stat. Assoc.* 63, 1379–1389. <https://doi.org/10.1080/01621459.1968.10480934>.
- Sneyers, R., 1992. On the use of statistical analysis for the objective determination of climate change. *Meteorol. Z.* 247–256. <https://doi.org/10.1127/metz/1/1992/247>.
- Soncini, A., Bocchiola, D., Azzoni, R., Diolaiuti, G., 2017. A methodology for monitoring and modeling of high altitude Alpine catchments. *Prog. Phys. Geogr. Earth Environ.* 41, 393–420. <https://doi.org/10.1177/0309133317710832>.
- Stucchi, L., Bombelli, G.M., Bianchi, A., Bocchiola, D., 2019. Hydropower from the Alpine Cryosphere in the Era of Climate Change: The Case of the Sabbione Storage Plant in Italy. *Water* 11, 1599. <https://doi.org/10.3390/w11081599>.
- Su, B., Xiao, C., Chen, D., Qin, D., Ding, Y., 2019. Cryosphere services and human well-being. *Sustainability* 11, 4365. <https://doi.org/10.3390/su11164365>.
- Tadono, T., Ishida, H., Oda, F., Naito, S., Minakawa, K., Iwamoto, H., 2014. Precise Global DEM Generation by ALOS PRISM. *ISPRS Ann. Photogramm. Remote Sens. Spat. Inf. Sci.* II 4, 71–76. <https://doi.org/10.5194/isprsannals-II-4-71-2014>.

- Terna, 2021. Dati Stat. Sull. 'Energ. Elettr. Ital. 2021.
- Terzago, S., Cassardo, C., Cremonini, R., Fratianni, S., 2010. Snow precipitation and snow cover climatic variability for the period 1971–2009 in the Southwestern Italian Alps: The 2008–2009 snow season case study. *Water* 2, 773–787. <https://doi.org/10.3390/w2040773>.
- Thackeray, C.W., Fletcher, C.G., Derksen, C., 2019. Diagnosing the impacts of northern hemisphere surface Albedo biases on simulated climate. *J. Clim.* 32, 1777–1795. <https://doi.org/10.1175/JCLI-D-18-0083.1>.
- Theil, H., 1992. A Rank-Invariant Method of Linear and Polynomial Regression Analysis. In: Raj, B., Koerts, J. (Eds.), *Henri Theil's Contributions to Economics and Econometrics: Econometric Theory and Methodology, Advanced Studies in Theoretical and Applied Econometrics*. Springer Netherlands, Dordrecht, pp. 345–381. https://doi.org/10.1007/978-94-011-2546-8_20.
- Valt, M., Cianfarra, P., 2010. Recent snow cover variability in the Italian Alps. In: *Cold Regions Science and Technology, International Snow Science Workshop 2009 Davos*, 64, pp. 146–157. <https://doi.org/10.1016/j.coldregions.2010.08.008>.
- Vanat, L., 2022. 2022 International Report on Snow & Mountain Tourism.
- Vicente-Serrano, S.M., Trambly, Y., Reig, F., González-Hidalgo, J.C., Beguería, S., Brunetti, M., Kalin, K.C., Patalen, L., Kržič, A., Lionello, P., Lima, M.M., Trigo, R.M., El-Kenawy, A.M., Eddenjal, A., Türkes, M., Koutroulis, A., Manara, V., Maugeri, M., Badi, W., Mathbout, S., Bertalanic, R., Bocheva, L., Dabanli, I., Dumitrescu, A., Dubuisson, B., Sahabi-Abed, S., Abdulla, F., Fayad, A., Hodzic, S., Ivanov, M., Radevski, I., Peña-Angulo, D., Lorenzo-Lacruz, J., Domínguez-Castro, F., Gimeno-Sotelo, L., García-Herrera, R., Franquesa, M., Halifa-Marín, A., Adell-Michavila, M., Noguera, I., Barriopedro, D., Garrido-Perez, J.M., Azorin-Molina, C., Andres-Martin, M., Gimeno, L., Nieto, R., Llasat, M.C., Markonis, Y., Selmi, R., Ben Rached, S., Radovanovic, S., Soubeyroux, J.-M., Ribes, A., Saidi, M.E., Bataineh, S., El Khalki, E.M., Robaa, S., Boucetta, A., Alsafadi, K., Mamassis, N., Mohammed, S., Fernández-Duque, B., Cheval, S., Moutia, S., Stevkov, A., Stevkova, S., Luna, M. Y., Potopová, V., 2025. High temporal variability not trend dominates Mediterranean precipitation. *Nature* 639, 658–666. <https://doi.org/10.1038/s41586-024-08576-6>.
- Wang, X., Xie, H., 2009. New methods for studying the spatiotemporal variation of snow cover based on combination products of MODIS Terra and Aqua. *J. Hydrol.* 371, 192–200. <https://doi.org/10.1016/j.jhydrol.2009.03.028>.
- Young, S.S., 2023. Global and regional snow cover decline: 2000–2022. *Climate* 11, 162. <https://doi.org/10.3390/cli11080162>.